A neutron powder diffraction determination of the thermal expansion tensor of crocoite ($PbCrO_4$) between 60 K and 290 K

KEVIN S. KNIGHT

ISIS Science Division, Rutherford Appleton Laboratory, Chilton, Didcot, Oxfordshire, OX11 0QX UK

Abstract

The thermal expansion tensor of crocoite has been determined from high-resolution neutron time-of-flight powder diffraction data. The temperature dependence of the lattice constants between 4.5 K and 290 K have been fitted to a quasi-harmonic Einstein model, and the temperature dependence of the thermal expansion tensor has been calculated for 60 K $\leqslant$ T $\leqslant$ 290 K. The magnitudes of the principal expansivities and their orientation exhibit saturation behaviour for temperatures above 300 K. The predicted saturated expansion coefficients are $\alpha_{11} = 33.1(1) \times 10^{-6}K^{-1}$, $\alpha_{22} = 15.72(3) \times 10^{-6}K^{-1}$, $\alpha_{33} = 3.36(1) \times 10^{-6}K^{-1}$, with α_{22} parallel to **b** and α_{11} lying at an angle of $-37.86(5)°$ to **c** for the $P2_1/n$ setting of the crystal structure. The direction of maximum expansion is approximately parallel to both $[10\bar{1}]$ and the least-squares line passing through the projection of the chromium atoms on (010). The direction of minimum expansion lies approximately parallel to [101]. No evidence was found for either a structural or magnetic phase transition between 4.5 K and 300 K.

KEYWORDS: crocoite, thermal expansivity, neutron diffraction, $PbCrO_4$.

Introduction

ALTHOUGH both chemically and structurally simple, the crystal structure of crocoite ($PbCrO_4$) was only fully determined in 1965 from a full three-dimensional analysis of Weißenberg data (Quareni and de Pieri, 1965). Earlier work had shown the space group to be $P2_1/n$ (Brill, 1931) with lattice constant ratios consistent with the morphological cell of Dauber (Palache *et al.*, 1951). Von Gliszczynski (1939) had shown that the crocoite was isomorphous with monazite from consideration of the lattice constants, and Brody (1942) located both heavy atoms from Patterson synthesis. The first full structure analysis was performed using two-dimensional projections of the electron density and suggested that the CrO_4^{2-} tetrahedron was significantly distorted (Quareni and de Pieri, 1964). Similar work was also carried out by Náray-Szabó and Argay (1965) who found to the contrary, that the tetrahedron was regular. This conclusion was later shown to be correct when the full three-dimensional data were subsequently analysed by Quareni and de Pieri. Since this work, there have been no further structure determinations of crocoite (Inorganic Crystal Structure Data release 9502) that improve on the precision of the light atom positional and thermal parameters.

Polymorphism has been reported in $PbCrO_4$, based on phase diagram studies (Jaeger and Germs, 1921), solid solution studies with SO_4^{2-}(Wagner *et al.*, 1932), and solution chemistry (Quittner *et al.*, 1932). The crystal structure of an orthorhombic polymorph was estimated from an X-ray powder data set, by analogy to anglesite, by Collotti *et al.* (1959), but its relation to the phase transitions detected by Jaeger and Germs is not clear. The only high-temperature data reported so far have been inconclusive but two structural phase transitions were found at approximately the temperatures reported by Jaeger and Germs; however, the powder patterns were neither interpreted nor in agreement with an anglesite structure type (Pistorius and Pistorius, 1962).

The unit cell volume of the orthorhombic polymorph is smaller than the room temperature

Mineralogical Magazine, December 1996, Vol. 60, pp. 963–972

volume of crocoite, which suggests that it might be a possible low-temperature or high-pressure phase which has been produced metastably from solution. However, the group relations between the space groups, for crocoite, $P2_1/n$, and anglesite, *Pnma*, suggests that it is more probably a high-temperature metastable phase; note that a high-temperature phase transition from the crocoite structure to the anglesite structure is known in $PbSeO_4$ (Popovkin and Simanov, 1962). To investigate the low-temperature option, powder diffraction data have been collected on natural crocoite between 4.5 K to 300 K. The powder diffraction data showed no evidence for either structural or magnetic phase transitions, and crystal structure refinement showed no major structural modifications between 4.5 K and room temperature (Knight, to be published). Although no structural changes were found, it was felt that the temperature dependence of the lattice constants might shed some light on the high temperature behaviour of $PbCrO_4$. The thermal expansion tensor of crocoite, determined from these data, is reported in this paper.

Experimental

A single crystal of crocoite from the Dundas mine, Tasmania, with an approximate volume of 1 cm^3 was lightly ground in an agate mortar and sieved to <75 μm. The powder was lightly packed in an aluminium can of slab geometry with thin vanadium front and back windows and a gadolinium absorbing mask screwed to the side of the can facing both the incident beam and the back scattering detectors. Heat could be supplied direct to the sample using a cartridge heater with maximum rating of 100 W placed in the side wall of the sample can. The temperature of the sample was measured using a Rh/Fe thermocouple mounted in the opposite wall of the can to the cartridge heater. The temperature of the sample was maintained using a Eurotherm controller under CAMAC control from a VAX3200 workstation. The sample can, heater and thermocouple were mounted on a centre stick and placed in a vanadium tailed ILL 'orange' cryostat. During data collections, the temperature measured was within 0.1 K of that requested and the temperature variation was less than 0.05 K.

Neutron time-of-flight powder diffraction data were collected on the high-resolution diffractometer HRPD (Johnson and David, 1985; Ibberson *et al.*, 1992) at the ISIS spallation source, Rutherford Appleton Laboratory. The 4.5 K data set was collected from 30000 μs to 230000 μs in time channel bins of $\Delta t/t = 1 \times 10^{-4}$, the time window corresponding to a *d*-spacing range of 0.6 Å to 4.6 Å in the back-scattering detector bank. All the intermediate temperature data collections were made with identical time channel binning but a time-of-flight range from 40000 μs to 140000 μs equating to a *d*-spacing range of 0.8 Å to 2.8 Å. Data collection times were 233 μAh for the 4.5 K data set and 10 μAh for all the intermediate temperatures. During data collection the effective beam current was 17 μA for the 4.5 K run and 34 μA for the intermediate temperature runs. The data collections from 10 K to 290 K were run by command file operation and included a 15 minute thermal equilibration step between the end of one run and the beginning of the next.

Data analysis

In a time-of-flight diffraction experiment, the neutron wavelength, λ, is related to the time-of-flight *t*, flight path *L*, neutron rest mass m_n and velocity *v* by

$$\lambda = h/m_n v = ht/m_n L$$

Substituting this expression into Bragg's law gives the relationship between time-of-flight and *d*-spacing.

$$d = ht/2m_n L\sin\vartheta$$

For HRPD the total flight path is 95.9647 m and the mean Bragg angle for the detector array is 168.329°, thus giving the conversion from time-of-flight to *d*-spacing as

$$d(\mathrm{m}) = 2.07182 \times 10^{-9} t(\mathrm{s}).$$

All data collections were made at the 1 m position of the diffractometer which gives an intrinsic resolution, full width at half maximum intensity, of $\Delta d/d = 8 \times 10^{-4}$ for the whole diffraction pattern.

Data normalising and fitting

All data sets were focussed to a Bragg angle of 168.329°, normalised to the incident monitor spectrum, background subtracted and corrected for detector efficiency using a diffraction pattern from vanadium. The data were corrected for wavelength dependent absorption in the vanadium tails of the cryostat as vanadium has a significant absorption cross section (508 fm^2 at λ = 1.798 Å; Sears, 1992). Finally the data were rebinned in $\Delta t/t = 3 \times 10^{-4}$ which represented the required resolution for the sample. After data reduction, data in the range of 45700 μs to 124365 μs were used for profile refinement.

Profile refinement was carried out by model independent fitting of the powder data using the program CAILS which is part of the time-of-flight least squares package REFINE (David *et al.*, 1992) based on the Rietveld method (Rietveld, 1967, 1969;

Young, 1993). The peak shape function used in the analysis was the convolution of a Voigt function, which models crystallite size and strain broadening, with two decaying exponentials, with differing time constants, and a switch function which take into account the effect of the moderator contribution (Ikeda and Carpenter, 1985). Profile analysis was carried out using the space group $P2_1/n$ with starting lattice constants from the work of Quareni and de Pieri (1965). Figure 1 shows the fit to the data collected at 4.5 K where the only significant features remaining in the difference plot are derived from unshielded parts of the aluminium sample can.

Temperature dependence of the lattice constants

The temperature dependence of the lattice constants are given in Table 1 and shown in Fig. 2. The data for all lattice parameters were fitted to the quasi-harmonic Einstein model used by David *et al.* (1993) in their study of the fullerene C_{60}, in which the temperature dependence of the cubic lattice constant was given by an equation of the form

$$\frac{(a - a(T = 0\text{K}))}{T} = \left(\frac{C_E}{T(\exp(\theta_E/T) - 1)}\right)$$

In this study of crocoite, a stands for any of the lattice constants, θ_E is an effective Einstein temperature and C_E is a constant. Although this model, which assumes a delta function in the phonon density of states at the Einstein frequency ω_E ($\hbar\omega_E = k_B\theta_E$), and is clearly a non-physical representation in this situation, the functional form of the temperature dependence of the lattice constant satisfies both the Grüneisen relation at low temperatures and becomes linear at higher temperatures. For $T \gg \theta_E$, the expansion coefficient becomes

$$\frac{1}{a_0}\frac{da}{dT} \approx \frac{C_E}{a_0\theta_E}$$

which is constant, and for $T \ll \theta_E$

$$\frac{1}{a_0}\frac{da}{dT} \approx \frac{C_E\theta_E}{a_0T^2\exp(\theta_E/T)}$$

in which the exponential term in the denominator dominates and hence the expression tends to zero as T becomes small. The data for each lattice constant were fitted to the full expression using least squares and the refined values of the 0 K lattice constant, Einstein constant and effective Einstein temperature are given in Table 2. Figure 2 shows the least squares fitted lines to the lattice constant data. With the exception of the c axis, the Einstein temperature is approximately constant at 126 K. For an Einstein oscillator, the Einstein frequency ω_E, and hence the Einstein temperature θ_E, is related to an effective restoring force constant and it is possible that the larger Einstein temperature in [001], and hence a stronger force constant, may reflect a greater hardness in crocoite in that direction (Abrahams and Bernstein, 1974).

Thermal expansivity

Until recently, diffraction determinations of thermal expansivities usually relied on the measurement of a

TABLE 1. Temperature dependence of the lattice constants for crocoite

Temp. (K)	a (Å)	b (Å)	c (Å)	β (degrees)
4.5(1)	7.08736(3)	7.40620(2)	6.76344(3)	102.0447(2)
10.0(1)	7.08721(21)	7.40638(11)	6.76353(22)	102.046(14)
30.0(1)	7.08818(22)	7.40669(12)	6.76382(23)	102.051(15)
50.0(1)	7.08984(22)	7.40801(12)	6.76486(23)	102.067(15)
70.0(1)	7.09186(22)	7.40968(12)	6.76614(23)	102.087(15)
90.0(1)	7.09430(22)	7.41141(12)	6.76797(23)	102.114(15)
110.0(1)	7.09680(22)	7.41350(12)	6.76996(23)	102.139(15)
130.0(1)	7.09975(22)	7.41526(12)	6.77249(25)	102.171(16)
150.0(1)	7.10257(22)	7.41752(12)	6.77498(25)	102.202(15)
170.0(1)	7.10522(22)	7.41973(13)	6.77778(25)	102.231(16)
190.0(1)	7.10821(22)	7.42197(13)	6.78043(27)	102.263(16)
210.0(1)	7.11125(22)	7.42446(12)	6.78321(26)	102.292(16)
230.0(1)	7.11440(23)	7.42682(14)	6.78634(30)	102.326(17)
250.0(1)	7.11786(24)	7.42891(13)	6.78933(32)	102.359(18)
270.0(1)	7.12080(25)	7.43161(13)	6.79248(34)	102.391(19)
290.0(1)	7.12380(31)	7.43377(16)	6.79559(34)	102.423(19)

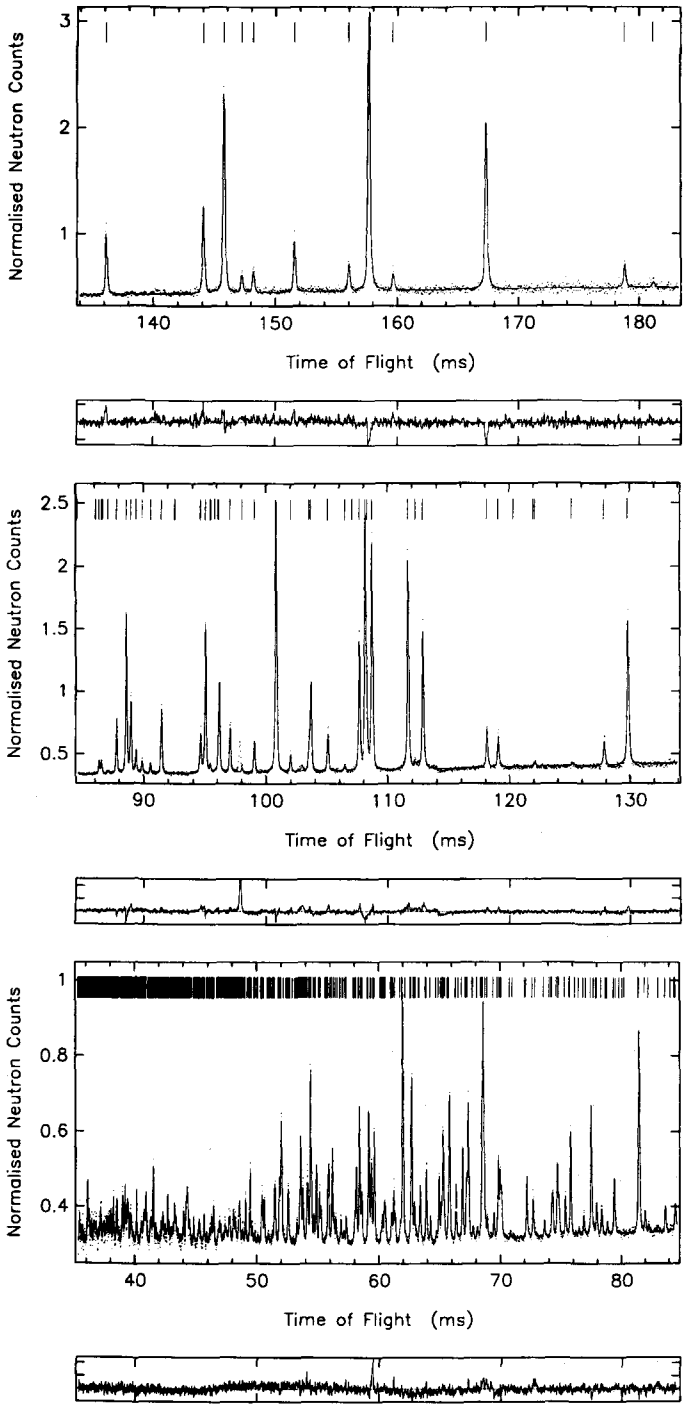

FIG. 1. Rietveld fit to crocoite at 4.5 K, observed (points), calculated (line) and difference/esd plot. Residual peaks derive from the aluminium sample can.

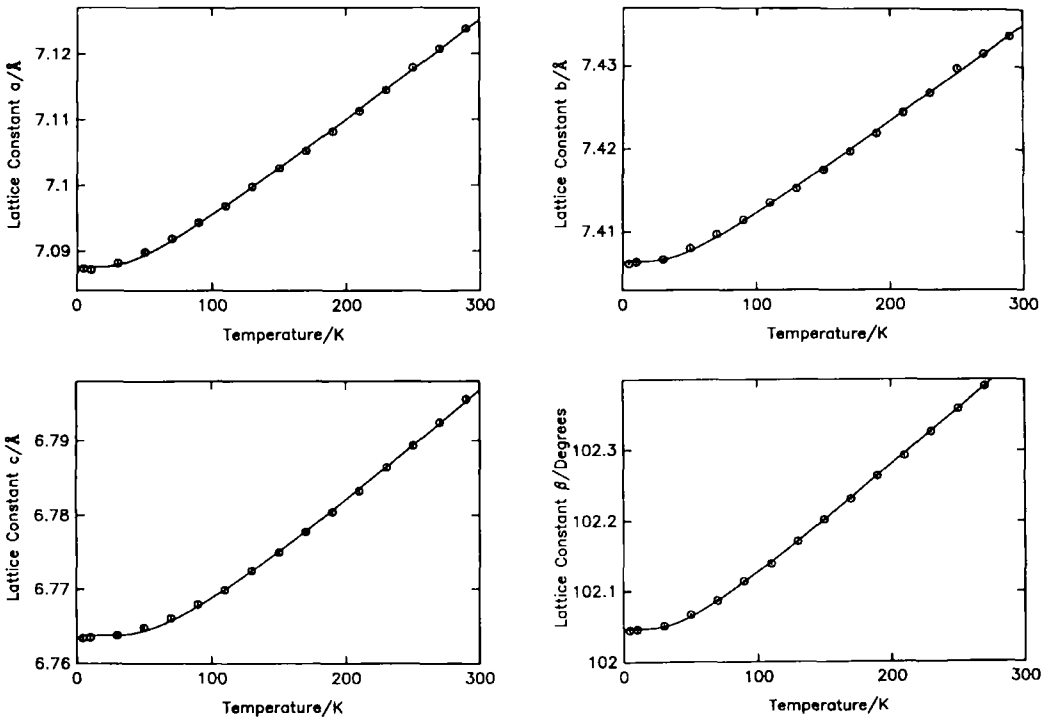

FIG. 2. The temperature dependence of the lattice constants of crocoite between 4.5 K and 290 K. Error bars are smaller than the plotting symbols in all cases. The calculated temperature dependence according to a quasi-harmonic Einstein model is shown as a full line.

limited set of diffraction vectors, a step of calculating the lattice constants from these diffraction vectors, and finally the substitution of the temperature dependence of the lattice constants into a set of formulae to determine the tensor components. This method has been recently criticised as reducing the precision in the measurement of the tensor components due to the step of calculating the lattice constants from the diffraction vectors (Jessen and Küppers, 1991). However, with the recent advances made in model independent fitting of the whole diffraction pattern for powder data, in which all reflections contribute to the lattice constant determinations, the lattice constants can be determined to far higher precision than the method that Jessen and Küppers propose where only a limited number of diffraction vectors are used. Indeed, in this work the precision of the lattice constants at 4.5 K is a factor of 100 better than their quoted esd's for the lithium hydrogen pthalate monohydrate used in their analysis. Hence for polycrystalline materials, powder diffraction data, in conjunction with profile fitting using the temperature dependence of the lattice constants, probably represents the optimum method for determining the thermal expansion tensor coefficients.

Thermal expansion tensor

Using the IRE (Institution of Radio Engineers) convention for the cartesian tensor basis: $\mathbf{e}_3 \parallel \mathbf{c}$, $\mathbf{e}_2 \parallel \mathbf{b}^*$, $\mathbf{e}_1 \parallel \mathbf{e}_2 \times \mathbf{e}_3$ (Jessen and Küppers, 1991), the thermal expansion tensor coefficients for a monoclinic crystal with b as the unique axis are related to the unit cell parameters by:

$$\alpha_{11} = \frac{1}{a_0 \sin\beta_0}\left[\sin\beta\frac{da}{dT} + a\cos\beta\frac{d\beta}{dT}\right]$$

$$\alpha_{22} = \frac{1}{b_0}\frac{db}{dT}$$

$$\alpha_{33} = \frac{1}{c_0}\frac{dc}{dT}$$

$$\alpha_{13} = \frac{1}{a_0}\frac{da}{dT}\left[\frac{1}{\sin 2\beta_0} - \frac{\sin\beta}{2\cos\beta_0}\right] - \frac{a\cos\beta}{2a_0\cos\beta_0}\frac{d\beta}{dT} - \frac{\cot\beta_0}{2c_0}\frac{dc}{dT}$$

Using the refined parameters from the least squares fit to the temperature dependence of the

TABLE 2. Least squares refined 0 K lattice constants, Einstein constants and Einstein temperatures for crocoite

Lattice parameter	Lattice constant at 0 K	Einstein constant (Å)	Einstein temperature (K)
a	7.0876(2) Å	$1.86(11) \times 10^{-2}$	121(7)
b	7.4064(2) Å	$1.53(11) \times 10^{-2}$	128(8)
c	6.7638(1) Å	$3.02(15) \times 10^{-2}$	195(7)
β	102.047(1)°	$2.10(7) \times 10^{-1}$	129(4)

lattice constants, the temperature dependence of the thermal expansion tensor was calculated from 4.5 K to 300 K using the above expressions. Figure 3 shows the calculated temperature dependence of the tensor coefficients which all exhibit the expected behaviour, essentially zero at very low temperatures and constant at higher temperatures.

Determination of principal axes and saturation behaviour

From the calculated values of the tensor components, the magnitudes of the principal axes were calculated for $T > 60$ K at seventeen temperatures using standard routines for eigenvector and eigenvalue determination. The results are given in Table 3 where it can be seen that there is a large anisotropy in the magnitudes of the principal axes. For $T > 60$ K there is an approximately 10:1 ratio in the magnitudes of the major:minor principal thermal expansivities, with the intermediate axis always lying parallel to **b**. At temperatures below 60 K all the values were found to be extremely small and are probably unreliable. Better estimates could possibly be determined by collecting data between 4.5 K and 100 K in smaller temperature intervals than used in this study. The temperature dependence of the magnitudes of the principal thermal expansivity coefficients and the

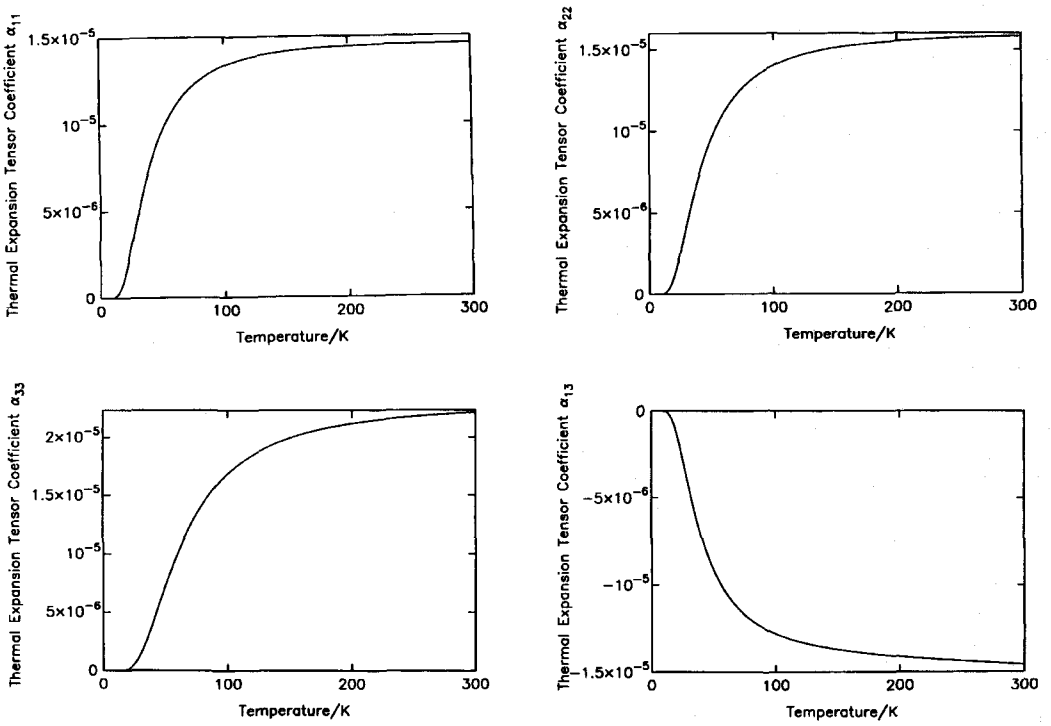

FIG. 3. Calculated temperature dependence of the thermal expansion tensor coefficients of crocoite.

TABLE 3. Calculated principal thermal expansion tensor coefficients ($\times 10^6$) and their orientation

Temp (K)	α_{33} (K^{-1})	α_{22} (K^{-1})	α_{11} (K^{-1})	Angle (degrees)
60.00	0.091	11.12	21.04	46.13
65.00	0.462	11.72	22.39	45.17
70.00	0.799	12.23	23.55	44.28
75.00	1.102	12.65	24.56	43.53
80.00	1.370	13.02	25.45	42.95
85.00	1.608	13.33	26.22	42.35
90.00	1.818	13.59	26.89	41.93
95.00	2.004	13.82	27.49	41.50
100.0	2.167	14.02	28.01	41.06
125.0	2.734	14.72	29.91	39.83
150.0	3.043	15.11	31.05	39.01
175.0	3.210	15.36	31.79	38.56
200.0	3.296	15.52	32.31	38.28
225.0	3.333	15.63	32.68	38.09
250.0	3.339	15.71	32.97	37.91
275.0	3.324	15.77	33.19	37.81
300.0	3.294	15.82	33.38	37.72

orientation in the *a–c* plane are shown in Fig. 4. The data clearly shows a move towards saturation for both the magnitudes and the orientation at a temperature slightly in excess of 300 K. The saturated principal expansivities and orientation were estimated by using least squares fitting to a simple exponential equation of the form

$$y = y_0 + A\exp(-T/B).$$

From the least squares fitting, the saturated thermal expansion coefficients were determined as $\alpha_{11} = 33.1(1) \times 10^{-6}K^{-1}$, $\alpha_{22} = 15.72(3) \times 10^{-6}K^{-1}$, $\alpha_{33} = 3.36(1) \times 10^{-6}K^{-1}$, with α_{22} parallel to **b** and α_{11} lying at an angle of $-37.86(5)°$ to **c** for the $P2_1/n$ setting of the crystal structure.

The direction of maximum expansion lies approximately in the $[10\bar{1}]$ direction for this setting of the crystal structure and is approximately parallel to the least squares line passing through the projection of the chromium atoms on to (010) which occurs at an angle of $-37.0(8)°$. The direction of minimum expansion is approximately parallel to [101]. The directions of the maximum and minimum expansion, the projection of the representation quadric and the crystal structure, viewed down **b**, are shown in Fig. 5. The orientation of the principal axes for these data were compared with that calculated from the only high-temperature cell parameter data for crocoite (Pistorius and Pistorius, 1962). Unfortunately the thermal expansion coefficients could only be calculated from a linear interpolation between two points, at 293 K and 883 K, and furthermore the precision of these measurements is poor. However, analysis of their data shows the magnitude of the maximum axis, $30 \times 10^{-6}K^{-1}$, is only slightly changed from the low-temperature study, and the orientation of this axis remains approximately along $[10\bar{1}]$. The magnitudes of the intermediate and minimum axes are both larger than the low-temperature investigation reported here.

Discussion and conclusions

Consideration of the group relationship between the space groups of the two polymorphs of $PbCrO_4$ with known crystal structure types, $P2_1/n$ and *Pnma*, suggests the possibility of a continuous second-order phase transition between the two phases occurring at high temperature. The simple argument based on the difference in unit cell volume between the two phases favouring the orthorhombic phase as a low-temperature polymorph has been shown to be incorrect from the results of the powder diffraction study presented here, although the possibility of it being a high-pressure phase cannot be discounted. Thermal analysis has shown the existence of two phase transitions in pure $PbCrO_4$ at 980 K and 1056 K (Jaeger and Germs, 1921), although the first was apparently absent when natural crocoite was measured. High-temperature *in-situ* X-ray diffraction found evidence for the first transition at 964 K and the second transition was inferred by quenching a

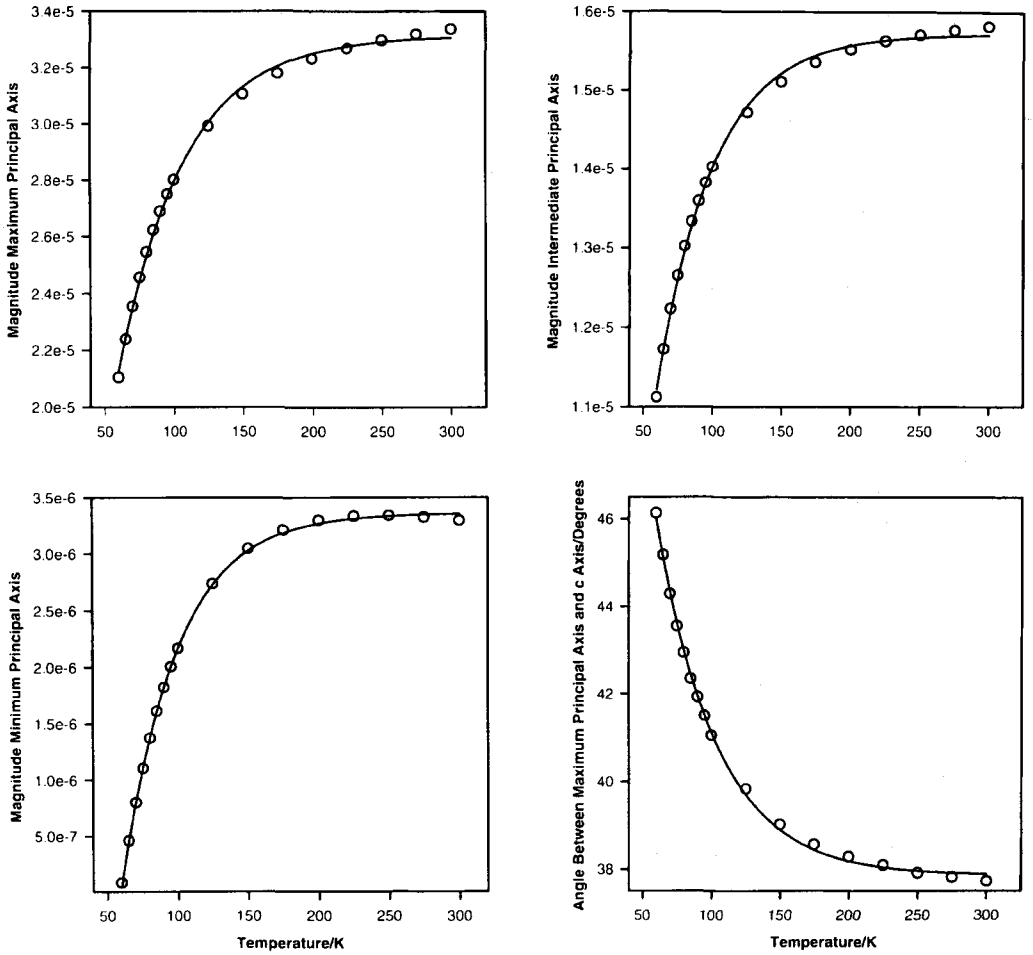

FIG. 4. The temperature dependence of the principal axis magnitudes and orientation for crocoite. The full line represents a fit to the data according to an exponential decay with temperature plus a saturation constant.

sample of $PbCrO_4$ from 1080 K (Pistorius and Pistorius, 1962). Neither of the X-ray diffraction patterns was consistent with an anglesite structure type and the phases remain uncharacterised, although the possibility of sample degradation due to oxygen loss which occurs at temperatures of the order of 873 K cannot be discounted (Pistorius and Pistorius, 1962). Nevertheless, if a high-temperature displacive transition is assumed, the application of Von Neumann's principle suggests that the $[10\bar{1}]$, [010] and [101] directions could become the crystallographic axes at the first phase transition, providing the cell becomes orthogonal. However, using the calculated thermal expansion coefficients to determine the temperature dependence of the angle between $[10\bar{1}]$ and [101] shows that this angle *decreases* away from 87.26° at 4.5 K with *increasing* temperature and minimises at approximately 200 K. The angle then increases with increasing temperature from 200 K, but only reaches 90° when extrapolated above the melting point. The magnitudes of the principal axes must therefore increase significantly from their room temperature values if they are to form the new cell edges at temperatures consistent with the phase transition temperatures. Furthermore, consideration of the crystal structures of crocoite and the anglesite structured phase show that a significant amount of shearing in the unit cell with associated rotations of the CrO_4^{2-} groups would be necessary for a displacive phase transition to occur between the

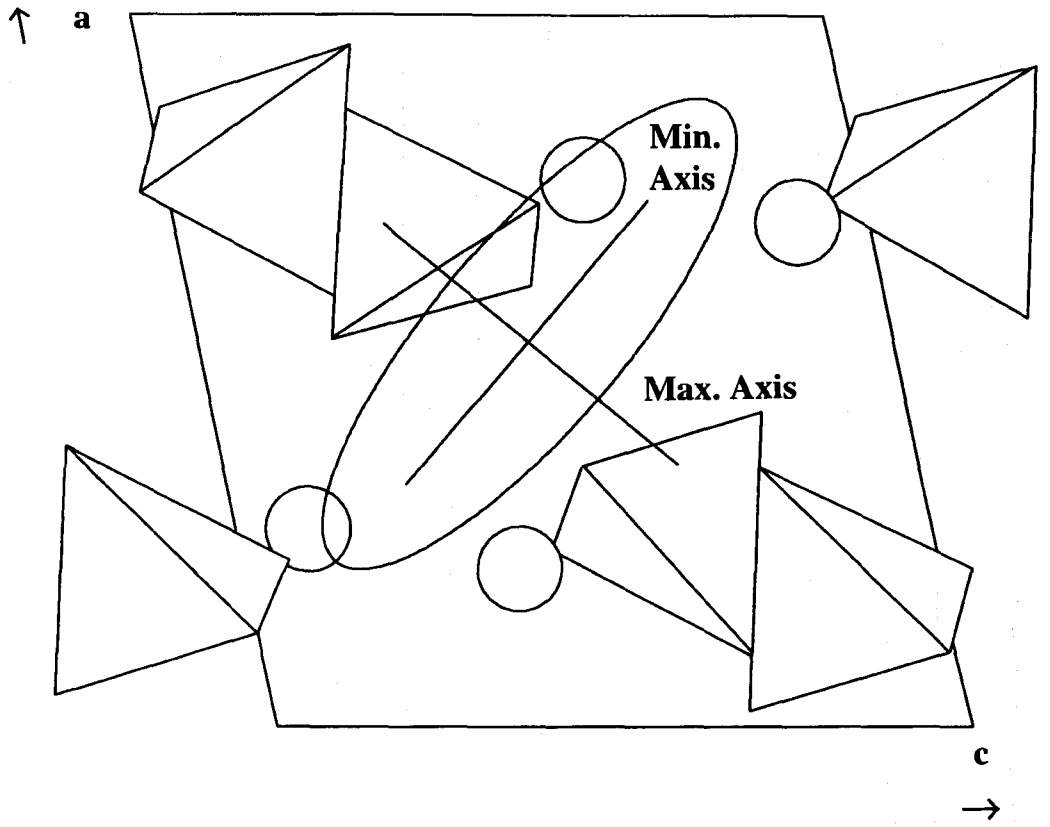

FIG. 5. The crystal structure and representation quadric for the saturated thermal expansion tensor of crocoite in the $P2_1/n$ setting viewed down the b axis. Lead atoms are circles and tetrahedra represent the CrO_4^{2-} groups.

two phases. Although it is clear that the major expansion along the line of the chromium atoms would allow freedom for the rotations to occur in the tetrahedral groups, the relationship of the crystal structures around a centre of symmetry strongly suggest that [10$\bar{1}$] and [101] are unlikely to form the cell edges if the phase transition to an anglesite structure occurs.

The nature of the high-temperature phases and any changes in the thermal expansion tensor with temperature are currently being investigated using neutron powder diffractometry.

Acknowledgements

I am grateful to Michael Henderson and Simon Redfern for their improvements to the manuscript and the editor is thanked for her patience in waiting for the revisions. My colleagues James Douglas and Michael Yates are thanked for the cryogenic support throughout the experiment.

References

Abrahams, S.C. and Bernstein, J.L. (1974) Piezoelectric nonlinear optic $CuGaSe_2$ and $CdGeAs_2$: crystal structure, chalcopyrite microhardness, and sublattice distortion. *J. Chem. Phys.*, **61**, 1140–6.

Brill, R. (1931) Über das gitter von bleichromat. *Zeit. Kristallogr.*, **77**, 506.

Brody, S.B. (1942) An X-ray investigation of the structure of lead chromate. *J. Chem. Phys.*, **10**, 650–2.

Collotti, G., Conti, L. and Zocchi, M. (1959) The structure of the orthorhombic modification of lead chromate $PbCrO_4$. *Acta Crystallogr.*, **12**, 416.

David, W.I.F., Ibberson, R.M. and Matthewman, J.C. (1992) Profile analysis of neutron powder diffraction data at ISIS. Rutherford Appleton Laboratory Report RAL-92-032.

David, W.I.F., Ibberson, R.M. and Matsuo, T. (1993) High resolution neutron powder diffraction: a case study of the structure of C_{60}. *Proc. Roy. Soc. Lond. A*, **442** 129–46.

Ibberson, R.M., David, W.I.F. and Knight, K.S. (1992) The high resolution powder diffractometer (HRPD) at ISIS — a user guide. Rutherford Appleton Laboratory Report RAL-92-031.

Ikeda, S. and Carpenter, J.M. (1985) Wide-energy-range, high-resolution measurements of neutron pulse shapes of polyethylene moderators. *Nuclear Instruments and Methods in Physics Research*, **A239**, 536–44.

Jaeger, F.M. and Germs, H.C. (1921) Über die binären systeme der sulfate, chromate, molybdate und wolframate des bleies. *Zeit. Anorg. Chem.*, **119**, 145–73.

Jessen, S.M. and Küppers, H. (1991) The precision of thermal-expansion tensors of triclinic and monoclinic crystals. *J. Appl. Crystallogr.*, **24**, 239–42.

Johnson, M.W. and David, W.I.F. (1985) HRPD: The high resolution powder diffractometer at the SNS. Rutherford Appleton Laboratory Report RAL-85-112.

Náray-Szabó, I. and Argay, G. (1965) Die krisrallstruktur des krokoits, $PbCrO_4$. *Acta Chimica Acad. Scientiarum Hungarae*, **40**, 283–8.

Palache, C., Berman, H. and Frondel, C. (1951) *The system of mineralogy of James Dwight Dana and Edward Salisbury Dana*, volume 2, 7th edition. John Wiley and Sons.

Pistorius, C.W.F.T. and Pistorius, M.C. (1962) Lattice constants and thermal-expansion properties of the chromates and selenates of lead, strontium and barium. *Zeit. Kristallogr.*, **117**, 259–71.

Popovkin, B.A. and Simanov, Y.P. (1962) An X-ray diffraction study of the two modifications of lead selenate. *Zh. Neorgan. Khim.*, **7**, 1743–4.

Quareni, S. and De Pieri, R. (1964) La struttura della crocoite, $PbCrO_4$. *Rendiconti della Societa Mineraloica Italiana*, **20**, 235–50.

Quareni, S., and De Pieri, R. (1965) A three-dimensional refinement of the structure of crocoite, $PbCrO_4$. *Acta Crystallogr.* **19**, 287–9.

Quittner, F., Sagpir, J. and Rassudowa, N. (1932) Die rhombische modifikation des bleichromates. *Zeit. Anorg. Chem.*, **204**, 315–7.

Rietveld, H.M. (1967) Line profiles of neutron powder-diffraction peaks for structure refinement. *Acta Crystallogr.*, **22**, 151–2.

Rietveld, H.M. (1969) A profile refinement method for nuclear and magnetic structures. *J. Appl. Crystallogr.*, **2**, 65–71.

Sears, V.F. (1992) Neutron scattering lengths and cross sections. *Neutron News*, **3**, 26–37.

Von Gliszczynski, S. (1939) Beitrag zur isomorphie von monazit und krokoit. *Zeit. Kristallogr.*, **101**, 1–16.

Wagner, H., Haug, R. and Zipfel, M. (1932) Die modifikation des bleichromats. *Zeit. Anorg. Chem.*, **208**, 249–54.

Young, R.A. (editor) (1993) *The Rietveld Method.* Oxford University Press.

[*Manuscript received 22 August 1994: revised 21 May 1996*]